Journal of Organometallic Chemistry 694 (2009) 1441–1446

Contents lists available at ScienceDirect

Journal of Organometallic Chemistry

journal homepage: www.elsevier.com/locate/jorganchem

Surveying the {AuCl} adducts of bulky phosphines bearing the 2,6-dimesitylphenyl group

David V. Partyka [a], Marlena P. Washington [b], James B. Updegraff III [b], Xufang Chen [b], Christopher D. Incarvito [c], Arnold L. Rheingold [c], John D. Protasiewicz [b,*]

[a] Creative Chemistry, LLC, Cleveland, OH 44106, USA
[b] Department of Chemistry, Case Western Reserve University, Cleveland, OH 44106, USA
[c] Department of Chemistry and Biochemistry, University of California at San Diego, La Jolla, CA 92093, USA

ARTICLE INFO

Article history:
Received 12 November 2008
Received in revised form 12 December 2008
Accepted 15 December 2008
Available online 31 December 2008

Keywords:
Phosphines
Phosphorus
Gold
Structure
Sterically hindered

ABSTRACT

A series of gold chloride {AuCl} adducts of the sterically demanding phosphines $DmpPR_2$ (Dmp = 2,6-dimesitylphenyl; R = H (**1**); Me (**2**); Cl (**3**)) have been prepared. The adducts are readily formed by the reaction of Au(tht)Cl and $DmpPR_2$, yielding [$(DmpPR_2)$AuCl] (R = H (**4**); Me (**5**); Cl (**6**)) in moderate to excellent yields. All three new compounds have been structurally characterized. The structures demonstrate little or no significant intermolecular Au···Au or intramolecular Au···arene interactions. In addition, the new difluoroarylphosphine $DmpPF_2$ (**7**) has been prepared and structurally characterized.

1. Introduction

Sterically encumbered organophosphorus compounds have attracted much attention, ranging from enabling the successful isolation of materials featuring novel multiply bonded low coordinate phosphorus centers [1,2] to providing unprecedented new catalytic applications for new forms of the "classic" R_3P phosphine ligands [3]. Despite being one of the older and most widely used ligands in inorganic chemistry, the careful design and study of new phosphines remains a prominent research theme in catalysis. For example, *ortho*-biphenyldialkylphosphine ligands have attracted attention for their ability to promote the highly efficient palladium-catalyzed CC coupling reactions of aryl halides with arylboronic acids [4]. Studies of such bulky phosphine ligands with late transition metals have resulted in the belief that these phosphine ligands enable the formation of palladium intermediates with low-coordination numbers at the metal center, possibly by stabilizing η^1 interactions of the metal atom with the *ipso* carbon of *ortho*-aryl arm on the biphenyl phosphine ligands. Our group has been interested in related phosphines carrying the terphenyl 2,6-$Mes_2C_6H_3$ (Dmp). The compound $DmpPCl_2$ (**3**, Chart 1, R = Cl) first reported by us in 1996 [5], has been proved useful for a variety of applications. This material serves as a convenient precursor to the phosphines $DmpPMe_2$ (**2**) [6] and $DmpPH_2$ (**1**) [5]. The former compound is an air stable phosphine with a high affinity for palladium, forming isolable complexes with palladium precursors. In the same investigation, it was reported that one of these palladium complexes, [$(DmpPMe_2)ClPd(\mu\text{-}Cl)]_2$, is a competent catalyst for the Suzuki coupling of hindered aryl chlorides and bromides with hindered boronic acids.

As we are interested in further refining our perception of the steric profiles of phosphines **1**–**3**, we have synthesized a series of three gold adducts of the form [$(DmpPR_2)$AuCl] to determine if these groups on phosphorus would have any effect on the manner in which gold is bound. Having two *ortho*-mesityl groups on each phosphine ensures the opportunity for each gold atom to engage in additional short Au···arene contacts, reminiscent of those postulated as being involved in low coordinate palladium chemistry. Short Au···arene contacts have often been noted in gold phosphine complexes [7–9]. In addition, other modes of reactivity are possible for halophosphines. For example, it has been reported that the phosphine diadamantylbenzylphosphine (Ad_2BnP) reacts with Au(tht)Cl to form an ion pair [$(Ad_2BnP)_2Au](AuCl)_2$ at room temperature; the gold atom of the cation has a weak (presumed) interaction with the pi face of each benzyl group [10]. Secondary interactions (aurophilic interactions) between gold atoms of neighboring complexes in the solid state offer additional diversity to the structures of gold phosphine complexes. Finally, we have prepared $DmpPF_2$ (**7**) as a new member of the of $DmpPR_2$ series and present its structure for comparison to the other materials.

* Corresponding author. Tel.: +1 216 368 5060; fax: +1 216 368 3006.
E-mail address: Protasiewicz@case.edu (J.D. Protasiewicz).

0022-328X/$ - see front matter © 2008 Elsevier B.V. All rights reserved.
doi:10.1016/j.jorganchem.2008.12.051

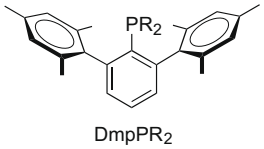

Chart 1.

2. Results and discussion

2.1. Synthesis

Compounds **1**–**3** were prepared as we have previously described. As has been demonstrated previously in the literature, Au(tht)Cl is a labile source of the {AuCl} fragment, and has been used successfully to aurate the bulky phosphines **1**–**3** to yield **4**–**6** in 46–85% yields. Reactions proceeded quickly at room temperature, and all three products were stable in the solid state in air for at least two days. Crystals of **5** appear to be stable in air for even longer periods. Scheme 1 illustrates the sequence of reactions.

Aryldifluorophosphines are less common compared to aryldichlorophosphines because of their instability towards redistribution to form bisarylfluorophosphines and phosphorus trifluoride, or redox disproportionation to form aryltetrafluorophosphoranes and cyclopolyphosphines [11–23]. $DmpPF_2$ (**7**), however, was isolated as a stable material by a chlorine–fluorine exchange reaction (Eq. (1))

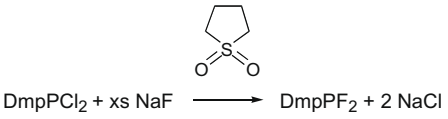

(1)

Thus a reaction mixture of $DmpPCl_2$, 10 equivalents of NaF and tetramethylene sulfone was heated to 120–130 °C for 45 min. The products were extracted with hexanes, followed by recrystallization to yield white crystals (74%) of **7**. The material was stable as a solid in air, but in chloroform solution underwent slow decomposition to unidentified materials.

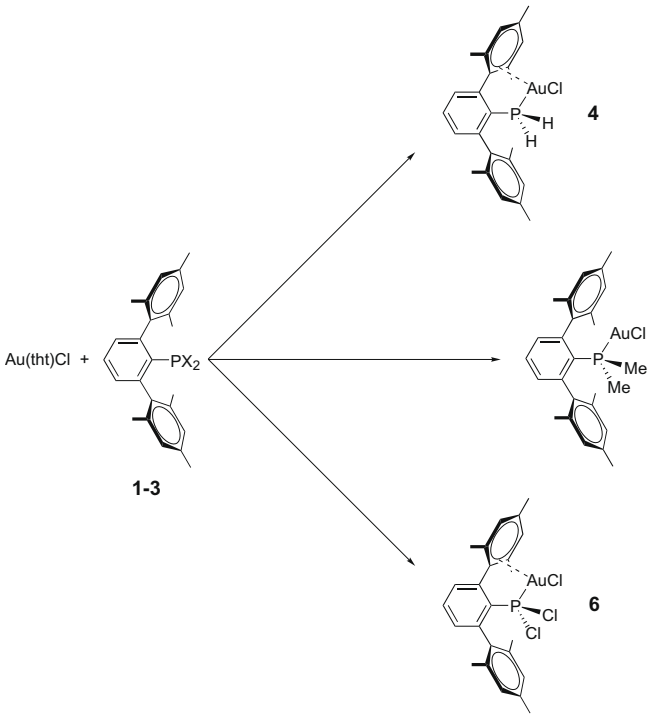

Scheme 1. Synthesis of $DmpP\{AuCl\}R_2$ complexes **4**–**6**.

2.2. NMR spectroscopy

All compounds were characterized by ^1H and $^{31}P\{^1H\}$ NMR spectroscopy. These gold complexes could adopt one of two idealized conformations about the P–C_{aryl} bonds (Chart 2). In conformer **A**, the gold atom lies above the mesityl ring and in a position to perhaps have close Au···C contacts. The contacts might be attributable to favorable Au···C interactions, or might the result of being forced into close proximity by steric clashes between the R groups and the other mesityl ring. In conformer **B**, the AuCl group is rotated by 90° about the P–C_{aryl} bond. In either conformation, one should expect to observe two sets of *ortho*-methyl resonances (a and a′), and for structure **A**, two sets of *para*-methyl resonaces (b and b′).

Like compounds **1**–**3**, however, compounds **4**–**6** display only two sets of mesityl CH_3 resonances in a 2:1 ratio (*a* and *b*, respectively) in their proton NMR spectra in $CDCl_3$ solution at room temperature. The ^1H NMR data does not distinguish between either conformer **A** or **B** and suggests facile rotation about the aryl-phosphorus bond (*vide infra*). If there are favorable contacts between the gold atom and mesityl ring carbon atoms, then the strength of possible attractions are not enough to hinder P–C_{aryl} bond rotation.

The $DmpPH_2$-gold adduct **4** features a prominent doublet at d 5.10 ppm attributable to the PH_2 protons ($^1J_{HP}$ 405 Hz). This data compares well to another sterically encumbered gold phosphine $Mes^*P\{AuCl\}H_2$ (d 5.52, $^1J_{HP}$ 402 Hz) [24]. The $DmpPMe_2$-gold adduct **5** likewise displays a doublet at d 1.20 attributable to the $P(CH_3)_2$ protons ($^2J_{HP}$ 10.4 Hz). The $^{31}P\{^1H\}$ NMR($CDCl_3$) resonances for **4**–**6** all appear as sharp singlets, suggesting that the Au–P bond is non-labile at room temperature. Relative to the free phosphine and upon gold adduct formation, the observed ^{31}P chemical shift is substantially downfield (>30 ppm) for **5**, but substantially upfield (>30 ppm) for **4** and **6**. A simple inductive effect explains this behavior for **5**, a pattern which has been repeatedly observed in the coordination chemistry of gold adducts of bulky, phosphorus containing ligands [7].

The ^{31}P NMR spectrum of **7** showed a triplet at δ 213.3 ppm ($^1J_{PF}$ = 1170 Hz) in $CDCl_3$. The ^{31}P NMR chemical shift and coupling constant are close to 2,6-dimethoxyphenyldifluorophosphine, δ 212.8 (t, $^1J_{PF}$ = 1160 Hz)[15,23] and is within the range of other published difluorophosphine compounds showing δ 197–216 ppm.

2.3. X-ray crystallography studies

The results of an X-ray structural determination on a single crystal of [($DmpPH_2$)AuCl] (**4**) is shown in Fig. 1. Molecules of **4** are loosely associated into dimers, where two PAuCl arrays are "sandwiched" or packed between two mesityl groups from each

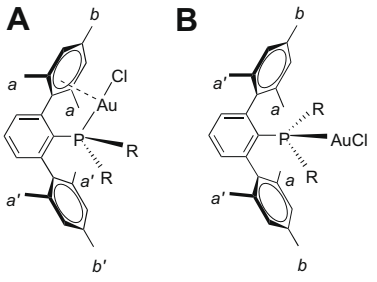

Chart 2.

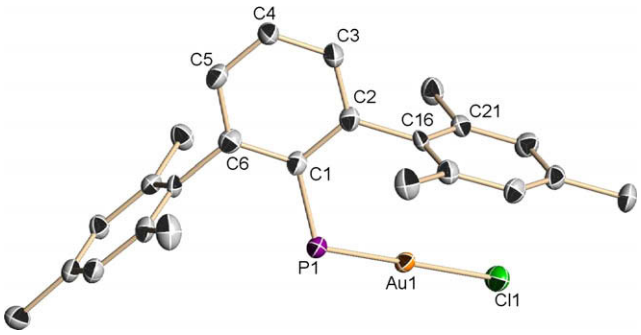

Fig. 1. ORTEP representation (showing 50% probability thermal ellipsoids) of **4**; hydrogen and disordered atoms have been omitted for clarity. Select bond distances (Å) and angles (°): Au1–P1, 2.222(1); Au1–Cl1, 2.281(4). P1–Au1–Cl1, 177.76(11); C2–C1–P1, 119.3(4); C6–C1–P1, 120.4(4). The closest Au···C contact is 3.14 Å.

molecule of **4** (Fig. 2). Interestingly, within this "dimer", there exists an 80/20 disorder of the AuCl units, giving rise to two conformers within the "sandwich" of flanking *ortho*-mesityl groups. The intermolecular Au–Au distances for each set of Au atoms is about 4.2 Å, too far to suggest any significant Au···Au interactions [25]. The disordered hydrogen atoms on the phosphorus atom were not located in the difference map. The two orientations of the AuCl vectors are rotated from the plane of the central phenyl ring by 40° (major) and 86° (minor), respectively. These conformers within the crystal represent conformers **B** (Chart 2) and something intermediate between **A** and **B**. Within the major isomer the closest Au···C contact is 3.14 Å. The Au–P distance of 2.222(1) Å is consistent with reported Au–P distances for bulky R_3PAuCl complexes [7].

The results of the structural determination of [(DmpPMe$_2$)AuCl] (**5**) is shown in Fig. 3. Crystals of **5** contain two independent molecules of **5**, as well as molecules of benzene trapped within the crystal (as also ascertained by ^{1}H NMR spectroscopy and elemental analysis data). As can be seen, **5** possesses approximate C_s symmetry, such that the plane containing the atoms Cl1, Au1, P1, and C3 bisects the molecule (akin to conformer **B**, Chart 2). Bond distances and angles for the gold atom are unexceptional, and the solid state conformation of **5** is almost identical with free phosphine **2** with one notable exception. In the crystal structure of **2** [6], one of the P–C_{Me} bond vectors essentially lies within the plane that bisects the central phenyl ring. However, to accommodate the {AuCl} fragment in **5**, the methyl groups (on phosphorus) assume positions such that the same plane bisects the C1–P1–C2 bond angle.

Fig. 4 presents the results of diffraction studies on [(DmpPCl$_2$)AuCl] (**6**). Interestingly, in the solid state compound **6** adopts a conformation **A** as portrayed in Chart 2. This orientation

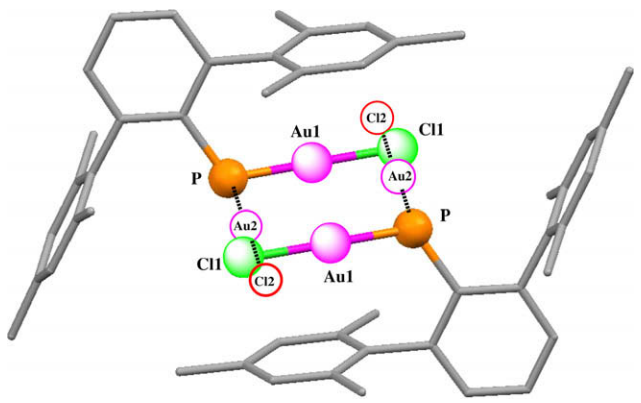

Fig. 2. Diagram showing loose association of **4** in the solid state and 80/20 disorder of AuCl units.

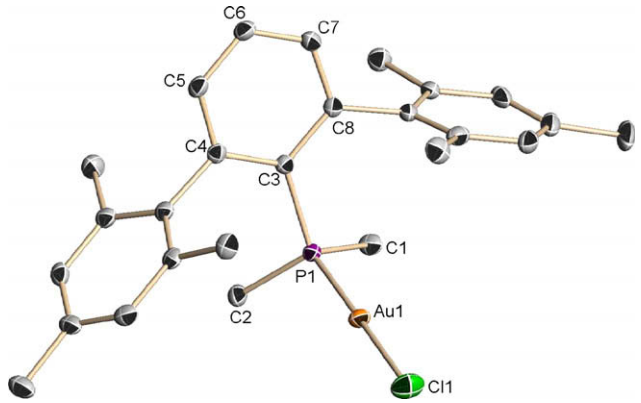

Fig. 3. ORTEP representation (showing 50% probability thermal ellipsoids) of one of two independent molecules of **5** · 1/2 C_6H_6; hydrogen atoms and benzene molecules of co-crystallization have been omitted for clarity. Selected bond distances (Å) and bond angles (°): Au1–P1, 2.2309(9); Au1–Cl1, 2.2964(10). P1–Au1–Cl1, 179.74(4); C3–P1–Au1, 113.37(1); C2–P1–C3, 109.25(2); C1–P1–C2, 99.44(2); C1–P1–C3, 109.64(2); C1–P1–Au1, 111.85(1); C2–P1–Au1, 112.40(1).

produces close contacts as short as 3.02 Å between the gold atom and carbon atoms of one flanking aryl group. With Au–C contacts under 3.2 Å as in the solid state structure of **6**, Au-η^2 (aryl) bonding interaction might be invoked, a phenomenon that has been observed previously [7,8]. The structure of the non-metallated DmpPCl$_2$ (**3**) was first mentioned by us [5], but never published owing to the fact that the structure was plagued by co-crystallization of the phosphinic acid DmpP(=O)(OH)(H) which led to erroneous P–Cl bond distances [26,27]. A better structure was later published [28], and like the related terphenyl 2,6-(*p*-*t*-BuC_6H_4)$_2$ $C_6H_3PCl_2$ it shows disparate C–C–P bond angles (20.2° and 16.8°, respectively) suggestive of attractions between the phosphorus atom and the p-system of the flanking aromatic group (so called Menshutkin interaction). We have, however, suggested an alternative proposal. Specifically, C–C–P angular distortions in 2,6-$Ar_2C_6H_3PR_2$ are attributable to repulsive forces between R groups on phosphorus and the flanking aryl rings that are forced into close proximity to one another [29]. It was thus of interest to examine another member of the series DmpPR$_2$, DmpPF$_2$ (**7**), where the phosphorus atom would have a very electronegative atoms of small steric profile. If attractive factors are responsible for asymmetric C–C–P bond angles in DmpPR$_2$, then in **7** should have even greater distortions.

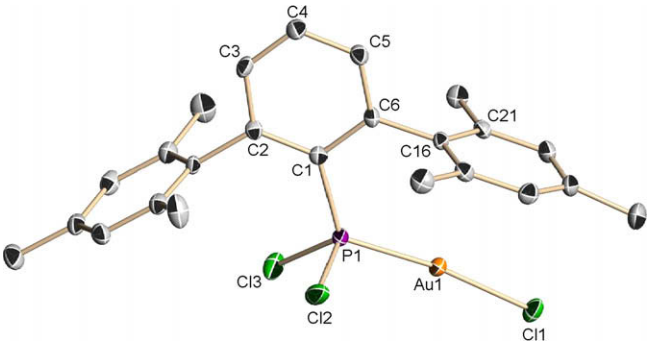

Fig. 4. ORTEP representation (showing 50% probability thermal ellipsoids) of **6**; hydrogen atoms have been omitted for clarity. Selected bond distances (Å) and bond angles (°): Au1–P1, 2.2070(7); Au1–Cl1, 2.2731(7); Au1–C16, 3.155; Au1–C21, 3.048. P1–Au1–Cl1, 172.94(2); C1–P1–Au1, 125.04(8); C1–P1–Cl2, 103.54(9); C1–P1–Cl3, 108.51(8); Cl2–P1–Cl3, 101.89(5); Cl2–P1–Au1, 107.96(4); Cl3–P1–Au1, 107.52(4). The closest Au···C contact is 3.02 Å.

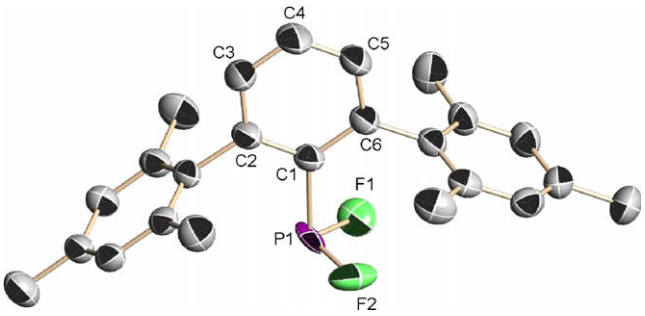

Fig. 5. ORTEP representation (showing 50% probability thermal ellipsoids) of **7**; hydrogen and disordered atoms have been omitted for clarity. Selected bond distances (Å) and bond angles (°): P1–F2, 1.488(3); P1–F1, 1.551(3); P1–C1, 1.898(3); F2–P1–F1, 103.4(2); F2–P1–C1, 100.9(1); F1–P1–C1, 97.9(1); C2–C1–P1, 114.7(1); C6–C1–P1, 125.3(2).

The structure of $DmpPF_2$ was thus determined (Fig. 5), and it reveals the presence of a positional disorder about the PF_2 unit. Two orientations, rotated by about 90° from one another and having the phosphorus atom displaced by 0.48 Å, were observed with occupancies at 65% and 35%. The bond lengths for P1–F1 and P1–F2 (major species) are slightly different with bond distances of 1.551(3) and 1.488(3) Å. The average bond phosphorus fluorine bond lengths are close to P–F bond lengths of 1.5814 (10) Å in $MesPF_2$ [30], and 1.572 and 1.581 (2) Å in an anthracene-9-PF_2 dimer [13]. The P–C bond length of 1.898 (3) and 1.785 (5) Å in the two orientations are comparable with the P–C bond length of 1.8116 (17) Å found for $MesPF_2$. The values are also consistent with those found in other terphenyl-substituted phosphines, for instance, 2,6-(*p*-*t*-$BuC_6H_4)_2C_6H_3PCl_2$ [1.837 (2), 1.833 (2) Å] [31]. The bond angles of C2–C1–P1 and C6–C1–P1 are 114.7(2)° and 125.2(2)°. The difference of 10.6° in bond angles, however, is smaller than that observed for 2,6-(*p*-*t*-$BuC_6H_4)_2C_6H_3PCl_2$ (16.8°), $DmpPCl_2$ (20.2°), and $DmpPMe_2$ (14.1°). The compounds having the larger two R groups and larger flanking aryl rings seem to produce the greatest differences in C–CP bond angles. The structural data are thus consistent with our previous arguments.

3. Conclusion

In summary, we have fully characterized three new $DmpPR_2$ gold complexes. Although the phosphorus atoms of the bulky phosphines **1**–**3** are the obviously binding sites for gold atoms, evidence accumulated in this investigation and others suggests that the pi face of the flanking aryl groups of the *meta*-terphenyl scaffold provides at best a weak additional binding site. Notably there exist a range of structural types for the series [$(DmpPR_2)$AuCl] that suggest rotation about the P–C_{aryl} bond is not difficult. In addition, the structure of $DmpPF_2$ provides additional insights into structural distortions that have been observed in *meta*-terphenylphosphines. The results of these studies suggest a range of conformations about the aryl-phosphorus bonds are accessible. Further studies are underway to examine the impact of other substituents on these types of complexes.

4. Experimental

All solvents and reagents were used as received. $DmpPH_2$ [5], $DmpPCl_2$ [5], and $DmpPMe_2$ [6] were synthesized according to the literature procedures. Tetrahydrothiophenegold(I) chloride was prepared according to the literature procedure [32]. Microanalyses (C, H, and N) were performed by Robertson Microlit Laboratories, Inc. All NMR spectra (^1H and $^{31}P\{^1H\}$) were recorded in $CDCl_3$ on a Varian AS-400 spectrometer operating at 399.7 and 161.8 MHz, respectively. Experiments involving manipulation of air- and water sensitive materials were carried out using Schlenk techniques or in a glove box under nitrogen. THF, hexanes, and diethyl ether were distilled from Na/benzophenone prior to use. The NMR spectroscopy measurements were recorded on a Varian Inova 400 spectrometer. Proton NMR chemical shifts were referenced to residual solvent signals.

4.1. [$(DmpPH_2)$AuCl] (**4**)

In a glovebox, $DmpPH_2$ (41 mg, 0.12 mmol) was dissolved in 2 mL of dichloromethane, and this solution was added dropwise to a solution of tetrahydrothiophenegold(I) chloride (37.9 mg, 0.12 mmol) in 2 mL of dichloromethane. The resultant solution was stirred for 20 min, and the solvent removed in vacuo. The residue was triturated with pentane and placed in a freezer in the glovebox. The spectroscopically pure white solid that separated was collected and dried. Yield: 58 mg (85%). A recrystallized sample (pentane/chlorobenzene) offered analytically pure material. ^1H NMR: δ 7.67 (t, 1H, *para*-$C_6H_3(Mes)_2$, J = 7.6 Hz), 7.24 (dd, 2H, *meta*-$C_6H_3(Mes)_2$, J = 4.0, 7.6 Hz), 7.02 (s, 4H, mesityl C*H*), 5.10 (d, 2H, $DmPH_2$, J = 405 Hz), 2.36 (s, 6H, *para*-mesityl CH_3), 2.05 (s, 12H, *ortho*-mesityl CH_3) ppm. $^{31}P\{^1H\}$ NMR: δ −85.4 (s, 1P) ppm. Anal. Calc. for $C_{24}H_{27}AuClP$: C, 49.80; H, 5.03. Found: C, 48.91; H, 4.70%.

4.2. [$(DmpPMe_2)$(AuCl)] · ½ C_6H_6 (**5** · ½ C_6H_6)

In a glove box, tetrahydrothiophenegold(I) chloride (61 mg, 0.19 mmol) was suspended in toluene (4 mL), and to this solution was added a 4 mL toluene solution of 1 equiv. (71 mg, 0.19 mmol) of $DmpPMe_2$. The resultant colorless solution was stirred for 2 h, and the solvent removed by rotary evaporation. The residue was triturated with pentane in air to liberate a colorless solid. The solid was recrystallized to afford colorless needles by vapor diffusion of pentane into a saturated benzene solution. NMR integration suggests approximately ½ molecule of benzene per molecule of **5**, and microanalysis confirmed this formulation. Yield: 88 mg (72%). ^1H NMR ($CDCl_3$): δ 7.56 (td, 1 H, *para*-$C_6H_3(Mes)_2$, J = 2.0, 7.6 Hz), 7.09 (dd, 2H, *meta*-$C_6H_3(Mes)_2$, J = 3.6, 7.6 Hz), 6.98 (s, 4H, mesityl C*H*), 2.37 (s, 6H, CH_3), 2.07 (s, 12 H, CH_3), 1.20 (d, 6H, $P(CH_3)$, J = 10.4 Hz) ppm. ^{31}P NMR ($CDCl_3$): δ −3.7 (s) ppm. Anal. Calc. for $C_{26}H_{31}AuClP \cdot ½\ C_6H_6$: C, 53.92; H, 5.31. Found: C, 53.49; H, 5.22%.

4.3. [$(DmpPCl_2)$AuCl] (**6**)

In a glove box, tetrahydrothiophenegold(I) chloride (37.5 mg, 0.12 mmol) was suspended in toluene (2 mL), and to this suspension was added a 3 mL toluene solution of 1 equiv. (48.6 mg, 0.12 mmol) of $DmpPCl_2$. The suspension quickly became a solution. After 2 h, the solution (with some orange precipitate) was evaporated to dryness in vacuo. The residue was extracted in air into a minimum of toluene, filtered through Celite, and pentane vapor was diffused to cause separation of large, colorless crystals. Yield: 35 mg (46%). ^1H NMR ($CDCl_3$): δ 7.75 (td, 1 H, *para*-$C_6H_3(Mes)_2$, J = 2.0, 7.6 Hz), 7.22 (dd, 2H, *meta*-$C_6H_3(Mes)_2$, J = 6.0, 7.6 Hz), 6.99 (s, 4H, mesityl C*H*), 2.39 (s, 6H, CH_3), 2.02 (s, 12H, CH_3) ppm. ^{31}P NMR ($CDCl_3$): δ 125.4 (s) ppm. Anal. Calc. for $C_{24}H_{25}AuCl_3P$: C, 44.50; H, 3.89. Found: C, 44.25; H, 3.73%.

4.4. $DmpPF_2$ (**7**)

A 50 mL round bottom flask was charged with 0.500 g (1.2 mmol) $DmpPCl_2$ and 0.543 g (12.9 mmol) sodium fluoride and equipped with a sealed condenser in the dry box, and then

Table 1
Crystallographic Data for **4**–**7**.

	4	**5**	**6**	**7**
Formula	$C_{24}H_{27}AuClP$	$C_{26}H_{31}AuClP \cdot 1/2\ C_6H_6$	$C_{24}H_{25}AuCl_3P$	$C_{24}H_{25}F_2P$
Formula weight	578.64	1291.97	647.73	382.41
Crystal system	Monoclinic	Monoclinic	Triclinic	Orthorhombic
Space group	*C*2/*c*	$P2_1/c$	$P\bar{1}$	*Pbca*
a (Å)	19.2941(17)	18.091(2)	8.6239(1)	17.799(12)
b (Å)	13.0939(17)	13.2710(2)	14.019(3)	7.845(5)
c (Å)	17.8329(18)	21.830(3)	20.921(5)	30.097(18)
α (°)	–	–	105.664(2)	–
β (°)	105.823(1)	93.585(1)	91.165(2)	–
γ (°)	–	–	100.477(2)	–
Cell volume (Å^3)	4334.5(8)	5230.8(1)	2388.5(8)	4203(5)
Z	8	4	4	8
$D_{calcd.}$ (mg m^3)	1.774	1.640	1.801	1.209
Temperature (K)	100(2)	100(2)	100(2)	218(2)
μ (mm^{-1})	6.991	5.803	6.571	0.153
F(000)	2256	2552	1256	1616
Crystal size (mm)	0.35 × 0.27 × 0.21	0.49 × 0.29 × 0.12	0.41 × 0.25 × 0.16	0.20 × 0.20 × 0.15
θ_{min}, θ_{max} (°)	2.08, 26.87	1.13, 27.20	1.01, 27.50	1.35, 28.29
No. of reflections collected	22847	58748	28576	29030
No. of independent reflections	4218	10050	9968	3556
No. of refined parameters	269	593	723	267
Goodness-of-fit on F^2[a]	0.819	1.055	1.016	1.342
R_1 [$I > 2\sigma(I)$][b]	0.0371	0.0274	0.0185	0.0665
wR_2 [$I > 2\sigma(I)$]	0.0402	0.0337	0.0214	0.0924
R_1 (all data)	0.1123	0.0627	0.0429	0.2109
wR_2 (all data)	0.1181	0.0661	0.0441	0.2295

[a] $GOF = [\sum w(F_o^2 - F_c^2)^2/(n-p)]^{1/2}$; *n* = number of reflections, *p* = number of parameters refined.
[b] $R_1 = \sum(||F_o| - |F_c||)/\sum|F_o|$; $wR_2 = [\sum w(F_o^2 - F_c^2)^2/\sum wF_o^4]^{1/2}$.

taken out of the dry box. To the mixture was added 5.2 mL of tetramethylene sulfone via syringe. The mixture was heated for 45 min with stirring and the temperature raised from room temperature to 130 °C. The mixture was cooled to room temperature to form a white gel-like material. The flask was taken into a dry box, where the mixture was extracted with three portions of hexanes. The clear solution was transferred to another clean flask. The solvent was evaporated under reduced pressure to one third volume, and the residue was recrystallized from hexanes to yield 0.48 g white crystalline solid (75%). The single crystals suitable for X-ray diffraction analysis were grown in hexane solution by slow evaporation. M.p. 213–215 °C. ^{1}H NMR ($CDCl_3$): δ 7.64 (t, J = 7.5 Hz, 1H), 7.12 (d, J = 6.6 Hz, 2H), 6.93 (s, 4H), 2.35 (s, 6H), 2.02 (s, 12H). ^{31}P {^{1}H} NMR ($CDCl_3$) δ: 213.3 (t, J = 1170 Hz). ^{19}F {^{1}H} NMR ($CDCl_3$) δ: −93.7 (d, J = 1170 Hz).

4.5. X-ray crystallographic studies

Crystals of **4** were grown by vapor diffusion of pentane into a saturated chlorobenzene solution (crystallographic information for **4** has been included in the supplementary material). Crystals of **5** were grown by vapor diffusion of pentane into a saturated benzene solution. Crystals of **6** were grown by vapor diffusion of pentane into a saturated toluene solution. Crystals of **7** were grown from hexane. Single crystal X-ray data were collected on a Bruker AXS SMART CCD diffractometers (for **4**–**6** at Case Western Reserve University and **7** at University of California, San Diego) using monochromatic Mo Kα radiation with omega scan technique. The unit cell was determined using APEX2 Crystallographic Suite. All structures were solved by direct methods and refined by full matrix least squares against F^2 with all reflections using SHELXTL. Refinement of extinction coefficients was found to be insignificant. All non-hydrogen atoms were refined anisotropically. All other hydrogen atoms were placed in standard calculated positions and all hydrogen atoms were refined with an isotropic displacement parameter 1.5 (CH_3) or 1.2 (all others) times that of the adjacent carbon or nitrogen atom. X-ray data collection and solution information is included as Table 1.

5. Supplementary material

CCDC 707819, 707820, 707817 and 707818 contain the supplementary crystallographic data for **4**, **5**, **6** and **7**. These data can be obtained free of charge from The Cambridge Crystallographic Data Centre via www.ccdc.cam.ac.uk/data_request/cif.

Acknowledgments

This work was supported by the National Science Foundation (CHE-0748982, and by CHE 0541766 for funds to for purchase of the X-ray diffractometer).

References

[1] B. Twamley, S.T. Haubrich, P. Power, Adv. Organomet. Chem. (1999) 1–65.
[2] J.A.C. Clyburne, N. McMullen, Coord. Chem. Rev. 210 (2000) 73–99.
[3] (a) A.F. Littke, G.C. Fu, Angew. Chem., Int. Ed. 41 (2002) 4176–4211;
(b) P. Van de Weghe, Lett. Org. Chem. 2 (2005) 113–117;
(c) U. Christmann, R. Vilar, Angew. Chem., Int. Ed. 44 (2005) 366–374;
(d) M. Miura, Angew. Chem., Int. Ed. 43 (2004) 2201–2203;
(e) R.B. Bedford, C.S.J. Cazin, D. Holder, Coord. Chem. Rev. 248 (2004) 2283–2321;
(f) H. Werner, Dalton Trans. (2003) 3829–3837.
[4] R. Martin, S.L. Buchwald, Acc. Chem. Res. 48 (2008) 1461–1473.
[5] E. Urnezius, J.D. Protasiewicz, Main Group Chem. 1 (1996) 369–372.
[6] R.C. Smith, R.A. Woloszynek, W. Chen, T. Ren, J.D. Protasiewicz, Tetrahedron Lett. 45 (2004) 8327–8330.
[7] D.V. Partyka, T.J. Robilotto, M. Zeller, A.D. Hunter, T.G. Gray, Organometallics 27 (2008) 28–32.
[8] Q.-S. Li, C.-Q. Wan, R.-Y. Zou, F.-B. Xu, H.-B. Song, X.-J. Wan, Z.-Z. Zhang, Inorg. Chem. 45 (2006) 1888–1890.
[9] E. Herrero-Gomez, C. Nieto-Oberhuber, S. Lopez, J. Benet-Buchholz, A.M. Echavarren, Angew. Chem., Int. Ed. 45 (2006) 5455–5459.
[10] U. Monkowius, M. Zabel, H. Yersin, Inorg. Chem. Commun. 11 (2008) 409–412.
[11] L. Heuer, M. Sell, R. Schmutzler, D. Schomburg, Polyhedron 6 (1987) 1295–1307.

[12] R. Bartsch, R. Schmutzler, G.U. Spiegel, O. Stelzer, J. Fluorine Chem. 36 (1987) 107–117.
[13] L. Heuer, D. Schomburg, R. Schmutzler, Chem. Ber. 122 (1989) 1473–1476.
[14] L. Riesel, J. Haenel, G. Ohms, J. Fluorine Chem. 38 (1988) 335–340.
[15] L. Heuer, R. Schmutzler, J. Fluorine Chem. 39 (1988) 197–216.
[16] F. Seel, K.H. Rudolph, Z. Anorg. Allg. Chem. 363 (1968) 233–244.
[17] H.G. Ang, R. Schmutzler, J. Chem. Soc. Sect. A: Inorg., Phys., Theor. (1969) 702–703.
[18] C. Brown, M. Murray, R. Schmutzler, J. Chem. Soc. Sect. C: Org. (1970) 878–881.
[19] E.L. Lines, L.F. Centofanti, Inorg. Chem. 12 (1973) 598–601.
[20] E.L. Lines, L.F. Centofanti, Inorg. Chem. 13 (1974) 2796–2799.
[21] E.L. Lines, L.F. Centofanti, Inorg. Chem. 13 (1974) 1517–1520.
[22] R. Schmutzler, O. Stelzer, J.F. Liebman, J. Fluorine Chem. 25 (1984) 289–299.
[23] L. Heuer, D. Schomburg, R. Schmutzler, Phosphorus, Sulfur Silicon Relat. Elem. 45 (1989) 217–222.
[24] H. Schmidbaur, G. Weidenhiller, O. Steigelmann, G. Mueller, Chem. Ber. 123 (1990) 285–287.
[25] H. Schmidbaur, Gold Bull. (London) 33 (2000) 3–10.
[26] G. Parkin, Chem. Rev. (Washington, DC, United States) 93 (1993) 887–911.
[27] G. Parkin, Acc. Chem. Res. 25 (1992) 455–460.
[28] D. Mootz, V. Haendler, Z. Anorg. Allg. Chem. 533 (1986) 23–29.
[29] R.C. Smith, S. Shah, E. Urnezius, J.D. Protasiewicz, J. Am. Chem. Soc. 125 (2003) 40–41.
[30] P.G. Jones, L. Heuer, R. Schmutzler, Acta Crystallogr., Sect. E: Struct. Rep. Online E58 (2002) o999–o1000.
[31] R.J. Wehmschulte, M.A. Khan, S.I. Hossain, Inorg. Chem. 40 (2001) 2756–2762.
[32] R. Uson, A. Laguna, M. Laguna, Inorg. Synth. 26 (1989) 85–91.